Hsp72 is targeted to the mitotic spindle by Nek6 to promote K-fiber assembly and mitotic progression

Laura O'Regan,[1] Josephina Sampson,[1] Mark W. Richards,[1] Axel Knebel,[2] Daniel Roth,[3] Fiona E. Hood,[4] Anne Straube,[3] Stephen J. Royle,[3,4] Richard Bayliss,[1] and Andrew M. Fry[1]

[1]Department of Biochemistry, University of Leicester, Leicester LE1 9HN, England, UK
[2]Kinasource Ltd, The Sir James Black Center, Dundee DD1 5EH, Scotland, UK
[3]Centre for Mechanochemical Cell Biology, Warwick Medical School, Coventry CV4 7AL, England, UK
[4]Department of Cellular and Molecular Physiology, University of Liverpool, Liverpool L69 3BX, England, UK

Hsp70 proteins represent a family of chaperones that regulate cellular homeostasis and are required for cancer cell survival. However, their function and regulation in mitosis remain unknown. In this paper, we show that the major inducible cytoplasmic Hsp70 isoform, Hsp72, is required for assembly of a robust bipolar spindle capable of efficient chromosome congression. Mechanistically, Hsp72 associates with the K-fiber–stabilizing proteins, ch-TOG and TACC3, and promotes their interaction with each other and recruitment to spindle microtubules (MTs). Targeting of Hsp72 to the mitotic spindle is dependent on phosphorylation at Thr-66 within its nucleotide-binding domain by the Nek6 kinase. Phosphorylated Hsp72 concentrates on spindle poles and sites of MT–kinetochore attachment. A phosphomimetic Hsp72 mutant rescued defects in K-fiber assembly, ch-TOG/TACC3 recruitment and mitotic progression that also resulted from Nek6 depletion. We therefore propose that Nek6 facilitates association of Hsp72 with the mitotic spindle, where it promotes stable K-fiber assembly through recruitment of the ch-TOG–TACC3 complex.

Introduction

Heat shock proteins (HSPs) are molecular chaperones that use ATP hydrolysis to aid the folding of nascent polypeptides, maintain proteins in unstable conformations, and prevent protein denaturation. These functions are essential in many biological contexts, including assembly of macromolecular complexes, protein trafficking, and regulation of enzyme activity (Bukau et al., 2006). HSPs are particularly important in cells subject to proteotoxic stress and are attracting considerable interest as potential targets for cancer therapy (Powers and Workman, 2007; Jego et al., 2013). The Hsp70 proteins represent a major family of HSPs that are frequently overexpressed in human cancers (Rohde et al., 2005; Daugaard et al., 2007; Kampinga and Craig, 2010). Their overexpression correlates with poor prognosis and drug resistance, whereas blocking Hsp70 function gives a therapeutic response in tumor models (Nylandsted et al., 2000; Schmitt et al., 2006; Leu et al., 2009; Massey et al., 2010; Powers et al., 2010; Rérole et al., 2011; Balaburski et al., 2013; Murphy, 2013).

In humans, there are eight canonical members of the Hsp70 family, as well as more distantly related members such as Hsp110 (Rohde et al., 2005; Daugaard et al., 2007). Some are expressed in a constitutive manner, such as Hsc70 (encoded by the *HSPA8* gene), whereas others are induced upon stress, such as Hsp72 (encoded by the *HSPA1A* gene). Rapidly dividing cancer cells frequently express high levels of both Hsc70 and Hsp72 as a result of oncogenic stress. Although some Hsp70 proteins are restricted to membranous compartments, such as Grp78/BiP in the endoplasmic reticulum and Grp75/mortalin in the mitochondria, Hsc70 and Hsp72 are present throughout the cytoplasm and nucleus. Hsp70 proteins also associate with the microtubule (MT) cytoskeleton, including the mitotic spindle, although to date, their only described function at this site is in protecting spindle pole integrity after heat shock (Liang and MacRae, 1997; Mack and Compton, 2001; Hut et al., 2005; Sauer et al., 2005; Elsing et al., 2014).

Correspondence to Andrew M. Fry: amf5@le.ac.uk

A. Knebel's present address is Medical Research Council Protein Phosphorylation Unit, The Sir James Black Center, Dundee DD1 5EH, Scotland, UK.

Abbreviations used in this paper: HSP, heat shock protein; IF, immunofluorescence; IP, immunoprecipitate; KESTREL, kinase substrate–tracking and elucidation; LSB, low salt buffer; MT, microtubule; NEBD, nuclear envelope breakdown.

The Rockefeller University Press $30.00
J. Cell Biol. Vol. 209 No. 3 349–358
www.jcb.org/cgi/doi/10.1083/jcb.201409151

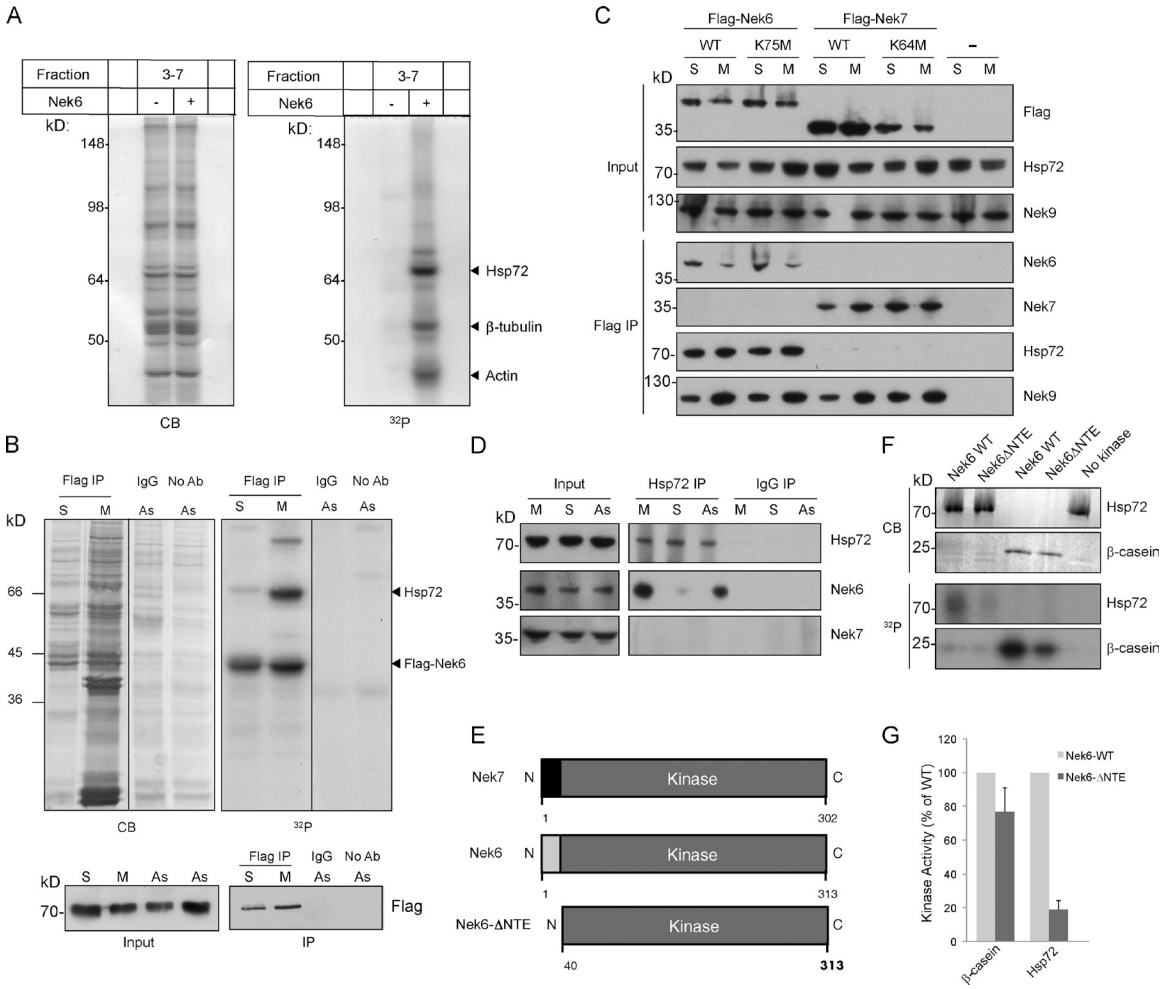

Figure 1. **Nek6 interacts with and phosphorylates Hsp72.** (A) KESTREL analysis of HEK 293 cytosolic extracts. Substrate-containing Superdex 200 fractions 3–7 were pooled, incubated with or without Nek6 and γ-[^{32}P]ATP, and analyzed by Coomassie blue stain (CB) and autoradiography (^{32}P). (B) Flag IPs were prepared from HEK 293 cells transfected with Flag-Nek6 and synchronized in S or M. As controls, asynchronous cells (As) transfected with Flag-Nek6 were subject to IP with rabbit IgGs or no antibodies (Ab). IPs were incubated with γ-[^{32}P]ATP before analysis by Coomassie blue stain and autoradiography (^{32}P). Lines have been added to top blots to indicate where intervening lanes were spliced out for presentation purposes. In A and B, molecular masses (kilodaltons) and proteins identified by mass spectrometry are indicated. (C) HEK 293 cells were transfected with wild-type (WT) or catalytically inactive (K75M and K64M) Flag-Nek6 or -Nek7 for 24 h before synchronization in S or M. Flag IPs were analyzed by Western blotting with the antibodies indicated. (D) Lysates (inputs), Hsp72 IPs, and IPs prepared with rabbit IgGs from asynchronous, S-phase, or M-phase arrested HEK 293 cells were analyzed by Western blotting with the antibodies indicated. (E) Schematic representation of Nek7, Nek6, and Nek6-ΔNTE. N, N terminus; C, C terminus. (F) In vitro kinase assays using purified wild-type Nek6, Nek6-ΔNTE, or no kinase with β-casein and Hsp72 protein substrates in the presence of γ-[^{32}P]ATP. (G) Substrate phosphorylation was quantified by scintillation counting of dried gels shown in F. Error bars show means ± SD.

Several members of the NEK protein kinase family contribute to mitotic progression (O'Connell et al., 2003; Quarmby and Mahjoub, 2005; Moniz et al., 2011; Fry et al., 2012). One of these is Nek6, which plays an essential role in spindle assembly and cytokinesis (Yin et al., 2003; O'Regan and Fry, 2009). Phosphorylation by Nek6 targets the Eg5/Kif11 motor protein to spindle MTs to promote centrosome separation (Rapley et al., 2008). However, this alone is unlikely to explain the fragile spindles and mitotic arrest that arise from blocking Nek6 function. Here, we show that Hsp72 is a novel mitotic substrate of Nek6 and that together these proteins play an essential role in assembly of robust mitotic spindles capable of efficient chromosome congression through K-fiber (kinetochore fiber) recruitment of the ch-TOG (colonic and hepatic tumor overexpressed protein) and TACC3 complex.

Results and discussion

Hsp72 is a novel mitotic substrate of the Nek6 kinase

To search for novel Nek6 substrates involved in spindle assembly, two approaches were used: a kinase substrate–tracking and elucidation (KESTREL) assay, which identifies proteins in fractionated cell extracts that act as excellent substrates for recombinant kinases in vitro (Cohen and Knebel, 2006), and a coprecipitation assay. The KESTREL screen identified Hsp72, β-tubulin, and actin as proteins that cofractionated through multiple steps of purification and were strongly phosphorylated by Nek6 (Fig. 1 A and Fig. S1). Hsp72 was also identified in Flag-Nek6 immunoprecipitates (IPs) prepared from mitotic cells and was strongly phosphorylated upon addition of ATP (Fig. 1 B).

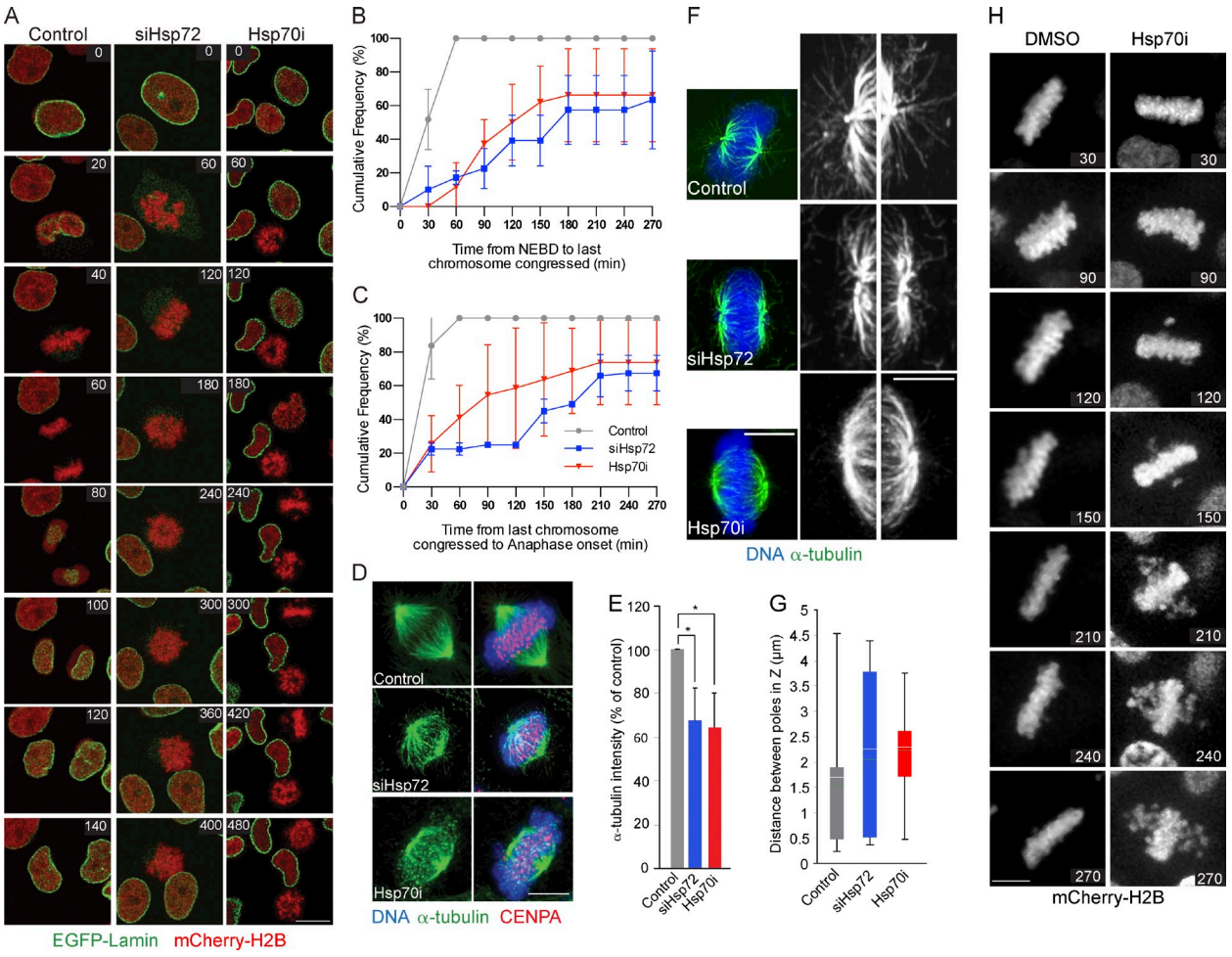

Figure 2. **Hsp72 promotes chromosomes congression and mitotic progression.** (A) HeLa:EGFP–lamin A/mCherry-H2B cells were either mock-depleted, depleted with siRNAs against Hsp72 for 72 h, or treated with Hsp70i for 4 h, as indicated, before time-lapse imaging. Stills from representative videos are shown with times (minutes) from mitotic entry indicated. (B and C) Quantification of cells from A indicating the time from NEBD to last chromosome congressed (B) and last chromosome congressed to anaphase onset (C). Data represent cumulative frequencies (±SD). (D) HeLa cells were mock depleted, depleted of Hsp72 for 72 h, or treated with Hsp70i for 4 h, as indicated, and then processed for IF with α-tubulin and CENP-A antibodies. (E) Total spindle MT intensity of cells in D was plotted relative to that of mock-depleted cells. *, $P < 0.05$. (F) HeLa cells treated as in D before IF with α-tubulin antibodies; enlargements show spindle pole regions. (G) Distance between spindle poles in the z axis of HeLa cells treated as in D. For box and whisker plots, boxes represent the 25th and 75th percentile, the green and white lines represent the medians and means, respectively, and whiskers show the 10th and 90th percentiles. (H) HeLa cells stably expressing mCherry-H2B were arrested in mitosis for 4 h with MG132. Time-lapse imaging was used to follow metaphase plate alignment with times (minutes) from addition of DMSO or Hsp70i as indicated. In D and F, DNA was stained with Hoechst 33258. Data are means (±SD) of 100–300 cells. Bars: (A, D, F [right], and H) 10 μm; (F, left) 2 μm.

Hsp72, identified using antibodies that do not cross-react with Hsc70 (Fig. S2 A), coprecipitated with wild-type and catalytically inactive Nek6 from S- and M-phase cells but not with the closely related Nek7 kinase (Fig. 1 C). In contrast, both Nek6 and Nek7 coprecipitated with their upstream activator, Nek9 (Roig et al., 2002).

Endogenous Nek6, but not Nek7, also coprecipitated with Hsp72, indicating that this interaction was not a result of Nek6 overexpression. Indeed, Nek6 coprecipitated more efficiently from cells arrested in M than S phase (Fig. 1 D). As Nek6 and Nek7 differ significantly only in the short (~30–40 amino acid) extensions N-terminal to the catalytic domains, a Nek6 truncation mutant lacking this N-terminal extension (Nek6-ΔNTE) was generated (Fig. 1 E). Although retaining significant activity against β-casein, truncated Nek6 barely phosphorylated Hsp72 (Fig. 1, F and G). This agrees with previous suggestions that the N-terminal extensions of these two kinases dictate their substrate specificity at least in the context of the full-length proteins (Richards et al., 2009; Vaz Meirelles et al., 2010). It also confirms that Nek6 and Nek7 almost certainly play distinct roles in cell division (O'Regan and Fry, 2009).

Hsp72 is required for spindle assembly and chromosome congression

To determine what function Hsp72 may have in mitotic progression in the absence of heat shock, it was depleted for 72 h with two independent siRNAs (Fig. S2 B) or inhibited for 4 h with the ATP-competitive small molecule, VER-155008 (Massey et al., 2010). HeLa cells were used for these experiments as they express high levels of Hsp72 (Rohde et al., 2005). Time-lapse imaging of EGFP–lamin A and H2B-mCherry revealed that depletion or inhibition of Hsp72 did not interfere with

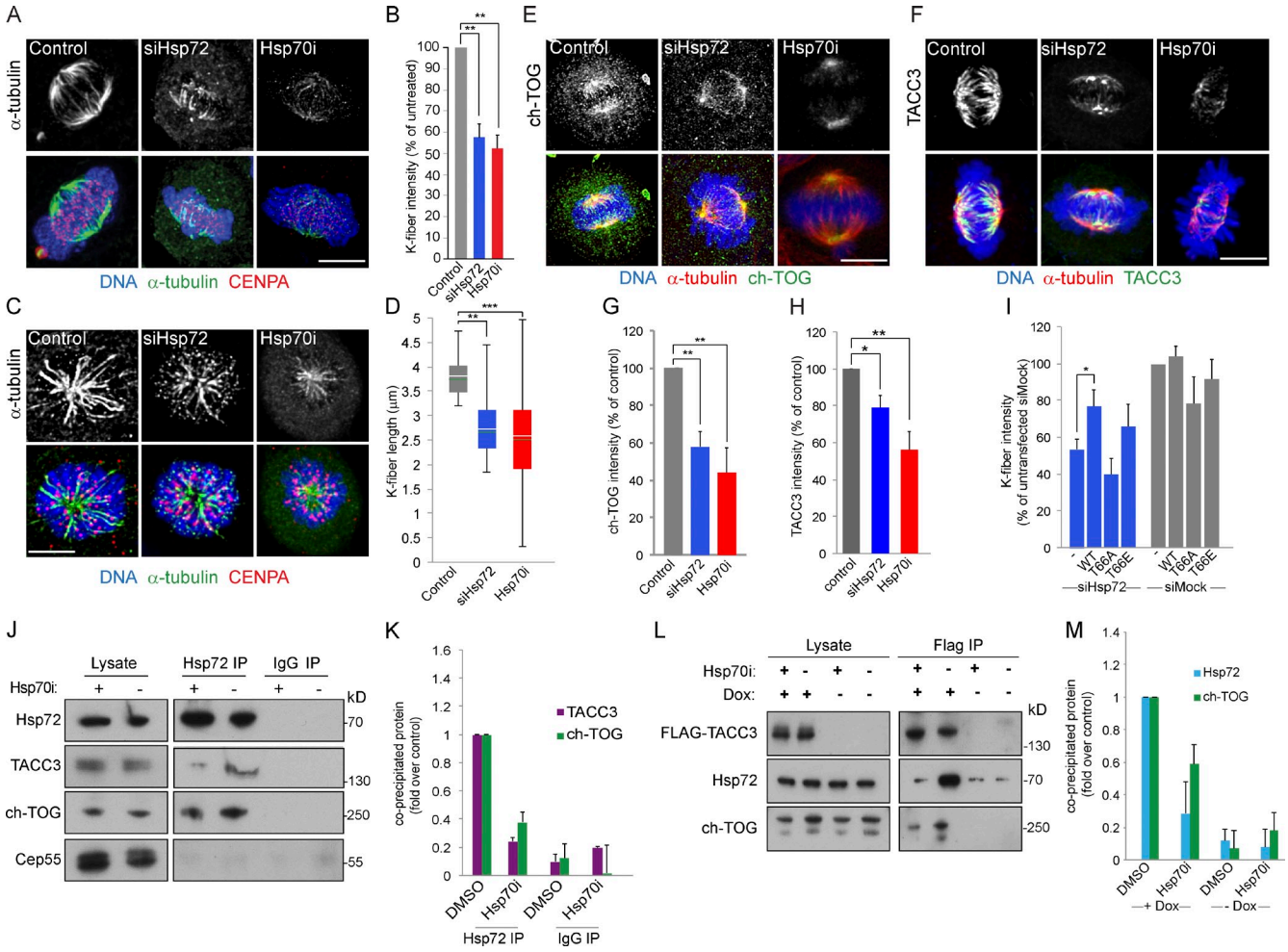

Figure 3. **Hsp72 promotes recruitment of ch-TOG–TACC3 complexes to K-fibers.** (A) HeLa cells treated as indicated were placed on ice for 10 min before IF with α-tubulin and CENP-A antibodies to reveal K-fibers. (B) K-fiber intensity is plotted relative to that in mock-treated cells. (C) HeLa cells treated as indicated were incubated with 50 μM monastrol for 4 h, placed on ice for 10 min, and then processed for IF with α-tubulin and CENP-A antibodies. (D) The length of K-fibers in the monopolar spindles is plotted. For box and whisker plots, boxes represent the 25th and 75th percentile, the green and white lines represent the medians and means, respectively, and whiskers show the 10th and 90th percentiles. (E and F) HeLa cells treated as indicated were processed for IF with antibodies against α-tubulin and ch-TOG (E) or TACC3 (F). (G and H) The intensity of ch-TOG (G) and TACC3 (H) relative to tubulin from cells in E and F is indicated. (I) K-fiber intensities were measured as in B after Hsp72 or mock depletion and expression of siRNA-resistant Hsp72 constructs. siMock, mock siRNA; WT, wild type. (J) Hsp72 IPs were prepared from mitotic cells treated with or without Hsp70i and analyzed by Western blotting with the antibodies indicated. (K) The amount of proteins precipitated in J is quantified relative to that in DMSO-treated Hsp70 IPs. (L) Flag IPs prepared from mitotic cells induced to express Flag-TACC3 with doxycycline and treated with Hsp70i were analyzed by Western blotting for Flag, Hsp72, and ch-TOG. (M) The amount of proteins precipitated in L is quantified relative to DMSO-treated Flag IPs. In A, C, E, and F, DNA was stained with Hoechst 33258. Data are means (±SD) of 100–300 cells. *, $P < 0.05$; **, $P < 0.01$; ***, $P < 0.001$. Bars, 10 μm.

chromatin condensation or nuclear envelope breakdown (NEBD). However, it strongly perturbed chromosome congression and anaphase onset (Fig. 2 A, Fig. S2 C, and Videos 1–3). In some cells, chromosomes rapidly detached from the metaphase plate, whereas in others, chromosomes failed to congress. Quantification confirmed that depletion or inhibition of Hsp72 extended the time in prometaphase by delaying the time from NEBD to last chromosome congressed and, in metaphase, by delaying the time from last chromosome congressed to anaphase onset (Fig. 2, B and C).

Staining of fixed cells with α-tubulin and CENP-A antibodies after either depletion or inhibition of Hsp72 revealed the presence of poorly organized spindles with reduced MT density (Fig. 2, D and E). A shortened interpolar distance, fewer astral MTs in the vicinity of poles and displacement of spindle orientation from the horizontal plane were also indicative of defective spindle–cortex attachment (Fig. 2, D, F, and G). Addition of the Hsp70 inhibitor to preformed spindles assembled in MG132-arrested mitotic cells led to release of chromosomes from the metaphase plate, indicating that Hsp70 is required to maintain, as well as establish, chromosome alignment (Fig. 2 H and Videos 4 and 5). Staining for the spindle assembly checkpoint protein, BubR1, revealed intense kinetochore staining upon either depletion or inhibition of Hsp72 (Fig. S2, D and E). Hence, Hsp72 is essential for HeLa cells to generate a robust mitotic spindle capable of cortical attachment, chromosome congression, and satisfaction of the spindle assembly checkpoint. Although the phenotypes of Hsp72 depletion and Hsp70 inhibition were remarkably similar, some differences were noted (e.g., more consistent displacement of spindle orientation in

Hsp70-inhibited cells; Fig. 2 G). This might reflect additional roles in mitosis for other Hsp70 isoforms inhibited by VER-155008.

Hsp72 promotes assembly of the ch-TOG–TACC3 complex and its recruitment to K-fibers

The chromosome congression defect points toward a failure to generate stable K-fibers, the MT bundles that attach spindle poles to kinetochores. Consistent with this, depletion or inhibition of Hsp72 led to a decrease in K-fiber intensity as visible in cold-treated cells (Fig. 3, A and B). Furthermore, K-fiber length in monopolar spindles assembled in the presence of the Eg5 inhibitor, monastrol, was reduced in the absence of functional Hsp72 (Fig. 3, C and D). To explore how Hsp72 might regulate K-fiber stability, localization of the ch-TOG and TACC3 proteins that contribute to inter-MT bridges in K-fibers was examined (Booth et al., 2011). Intriguingly, blocking Hsp72 function led to loss of both proteins from the mitotic spindle (Fig. 3, E and F). This loss of K-fiber association was greater than loss of K-fibers themselves, as revealed by measuring abundance relative to tubulin (Fig. 3, G and H), and could be rescued by expression of RNAi-resistant Hsp72 (Fig. 3 I and Fig. S2 F). K-fiber association of ch-TOG and TACC3 depends on their assembly into a complex that also includes clathrin (Hood et al., 2013). Endogenous Hsp72 coprecipitated from mitotic cells with TACC3 and ch-TOG but not the spindle-associated Cep55, whereas their association with Hsp72, but not their expression, was diminished upon loss of Hsp70 function (Fig. 3, J and K; and Fig. S2 G). Moreover, interaction between Flag-TACC3, expressed in doxycycline-inducible cells, and both Hsp72 and ch-TOG was perturbed in mitotic cells by the Hsp70 inhibitor (Fig. 3, L and M). Thus, we propose that Hsp72 contributes to robust spindle assembly through promoting ch-TOG–TACC3 complex formation and K-fiber recruitment, although we do not rule out additional roles in spindle MT assembly or stability.

Phosphorylation by Nek6 targets Hsp72 to the mitotic spindle

To determine how Nek6 regulates Hsp72, the endogenous Hsp72 protein purified in the KESTREL screen was incubated with Nek6 in vitro and subjected to mass spectrometry. This identified Thr-66, which lies within the N-terminal nucleotide-binding domain and is conserved across the human Hsp70 isoforms, as a major phosphorylation site (Fig. 4 A and Fig. S3, A and B). Mutation of this site to alanine (T66A) led to substantial loss of phosphorylation by Nek6 in vitro (Fig. S3 C). A phosphospecific antibody (pHsp70) generated against this site detected recombinant wild-type Hsp72, but not a T66A mutant, after incubation with Nek6 (Fig. 4 B). Western blotting with the pHsp70 antibody of IPs prepared with Hsp72 antibodies demonstrated that both endogenous and recombinant Hsp72 were phosphorylated on this site in mitosis, whereas pHsp70 reactivity was lost in cells depleted of Nek6 (Fig. 4, C–E). Hence, we conclude that Hsp72 is phosphorylated on Thr-66 in a mitosis-specific and Nek6-dependent manner.

Consistent with identification of Hsp70 proteins in purified human spindle preparations (Mack and Compton, 2001; Sauer et al., 2005), Hsp72 antibodies stained spindle MTs in HeLa cells, particularly in the vicinity of spindle poles in early mitosis before concentrating at the midbody in late mitosis (Fig. 4 F). This staining was lost upon Hsp72 depletion (Fig. S2 H). Recombinant wild-type and catalytically inactive (K71E) Hsp72 proteins also localized to spindle MTs in HEK 293 cells, indicating that catalytic activity is not required for spindle association (Fig. 4 G). The pHsp70 antibody revealed no staining of interphase cells, consistent with low Nek6 activity outside of mitosis but strongly stained spindle poles and sites of MT–kinetochore attachment in metaphase cells (Fig. 4 H). Again, this staining was lost upon depletion of Hsp72 (Fig. S3 D). Close inspection revealed spatially distinct localization of pHsp70 and the inner kinetochore marker, CenpA, but strong coherence with the outer kinetochore marker, CenpE (Fig. 4 I). Together with the presumed defects in spindle–cortex attachment seen upon loss of Hsp72 function, this might suggest additional, as-yet-undetermined, roles in attachment of MT plus ends to kinetochores and the cortex. Strikingly, depletion of Nek6 led to loss of Hsp72 from the mitotic apparatus that was above and beyond the reduced MT density that results from Nek6 depletion (Fig. 4, J and K). We therefore conclude that phosphorylation by Nek6 contributes to spindle localization of Hsp72 during mitotic progression.

A phosphomimetic Hsp72 mutant can rescue mitotic defects caused by Nek6 depletion

To determine whether the mitotic progression defects seen upon Nek6 depletion (Yin et al., 2003; O'Regan and Fry, 2009) might result from failure to phosphorylate Hsp72, wild-type and mutant Hsp72 proteins were expressed in cells from which Nek6 had been depleted (Fig. S2 I). Wild-type Hsp72 and the T66A mutant were unable to rescue the increase in mitotic index induced by Nek6 depletion; however, this was rescued by Hsp72-T66E (Fig. 5 A). Interestingly, expression of the T66A mutant in mock-depleted cells led to a twofold increase in the mitotic index, and microscopic analysis revealed a significant increase in multinucleated cells and cells with chromatin bridges and micronuclei indicative of mitotic failure (Fig. 5 B). K-fiber intensities and spindle recruitment of ch-TOG and TACC3 were also reduced in Nek6-depleted cells in a manner similar to that seen upon Hsp72 depletion (Fig. 5, C–H). This reveals for the first time that Nek6 contributes to K-fiber stability and ch-TOG/TACC3 recruitment. Moreover, Hsp72-T66E, but not wild-type Hsp72, could rescue the loss of K-fibers and ch-TOG/TACC3 recruitment in Nek6-depleted cells. In contrast, the T66A mutant failed to effectively localize to the spindle and exacerbated the K-fiber and ch-TOG/TACC3 recruitment defect in cells depleted of Nek6. It was also unable to rescue the K-fiber defect seen upon Hsp72 depletion (Fig. 3 I). We therefore conclude that Hsp72 represents an important new target of Nek6 and that Nek6 function in spindle assembly is, at least in part, exerted through phosphorylation of Hsp72.

This study identifies Hsp72 as an essential regulator of cancer cell division. HSP inhibitors are being developed as anticancer drugs with Hsp90 inhibitors in advanced clinical trials

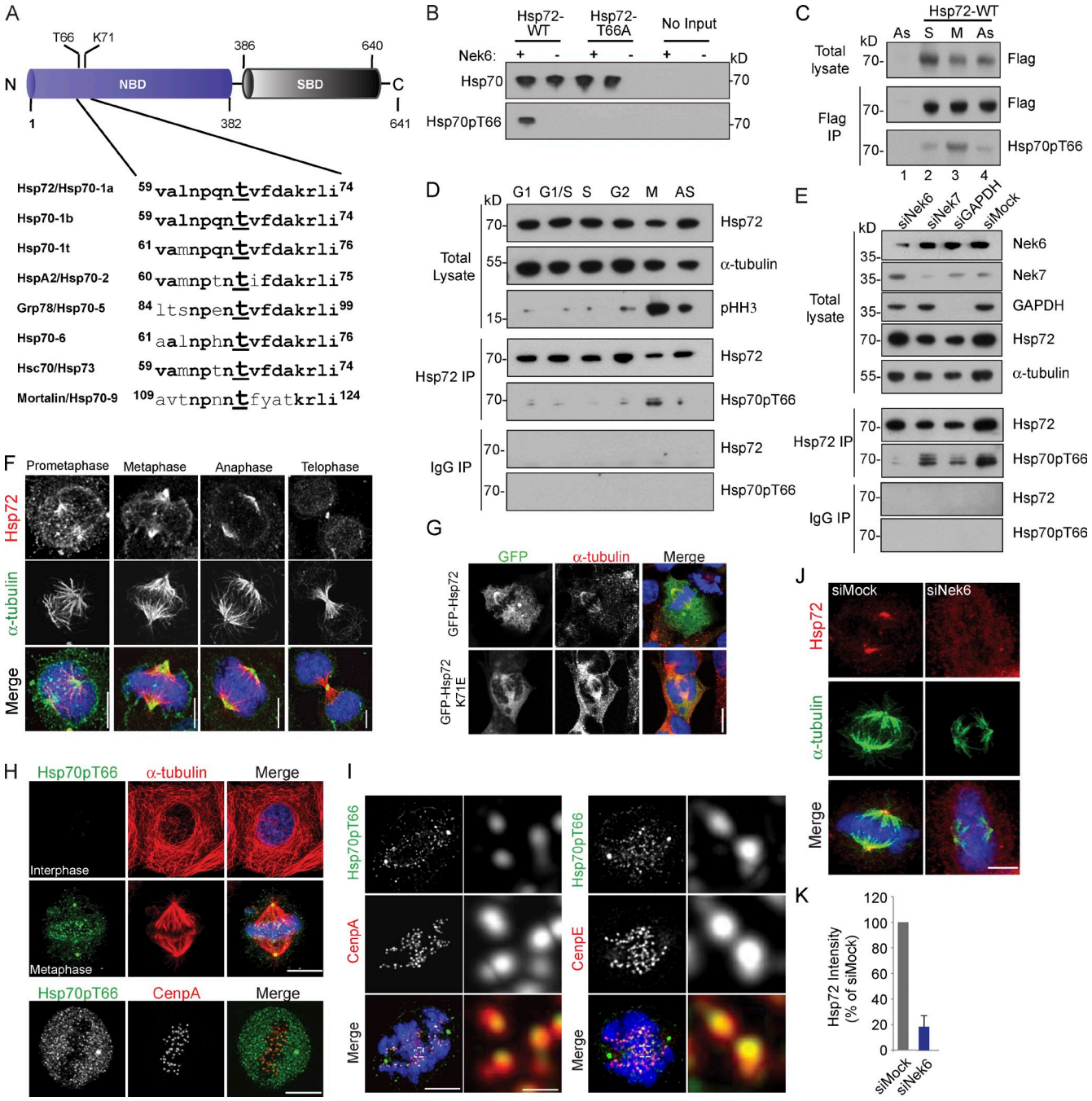

Figure 4. **Nek6 phosphorylation targets Hsp72 to the mitotic spindle.** (A) Schematic representation of Hsp72 showing nucleotide (NBD) and substrate (SBD) binding domains and sequence alignment of the human Hsp70 family around threonine-66. Bold indicates conserved residues. N, N terminus; C, C terminus. (B) Purified Hsp72 wild-type (WT) or T66A proteins incubated with or without purified Nek6 were subjected to Western blotting with total Hsp70 and Hsp70-pT66 (pHsp70) antibodies (C) HEK 293 cells were either untransfected (lane 1) or transfected with Flag-Hsp72 wild type (lanes 2–4) and left asynchronous (As) or synchronized at S or M before immunoprecipitation with Flag antibodies. Lysates and Flag IPs were analyzed by Western blotting with Flag and pHsp70 antibodies. (D) Lysates and Hsp72 IPs from HEK 293 cells that were either asynchronous or synchronized in different cell cycle stages were analyzed by Western blotting as indicated (pHH3, phospho–histone H3). (E) Lysates and Hsp72 IPs from HEK 293 cells transfected with Nek6, Nek7, or GAPDH siRNAs were analyzed by Western blotting as indicated. (F) HeLa cells were processed for IF with α-tubulin and Hsp72 antibodies. (G) HEK 293 cells transfected with GFP-tagged wild-type and catalytically inactive (K71E) Hsp72 were analyzed by IF with α-tubulin (red) and GFP (green) antibodies. (H and I) HeLa cells were processed for IF with pHsp70 and α-tubulin, CenpA, or CenpE antibodies, as indicated. In I, zoomed-in views of kinetochores are shown on the right from the boxed regions in the cells on the left. (J) HeLa cells were mock- or Nek6-depleted before IF with Hsp72 and α-tubulin antibodies. (K) The intensity of Hsp72 at metaphase spindle poles was quantified relative to α-tubulin. In F–J, DNA was stained with Hoechst 33258 (blue). siMock, mock siRNA. Bars: (F–I [left images] and J) 10 µm; (I, right images) 0.5 µm.

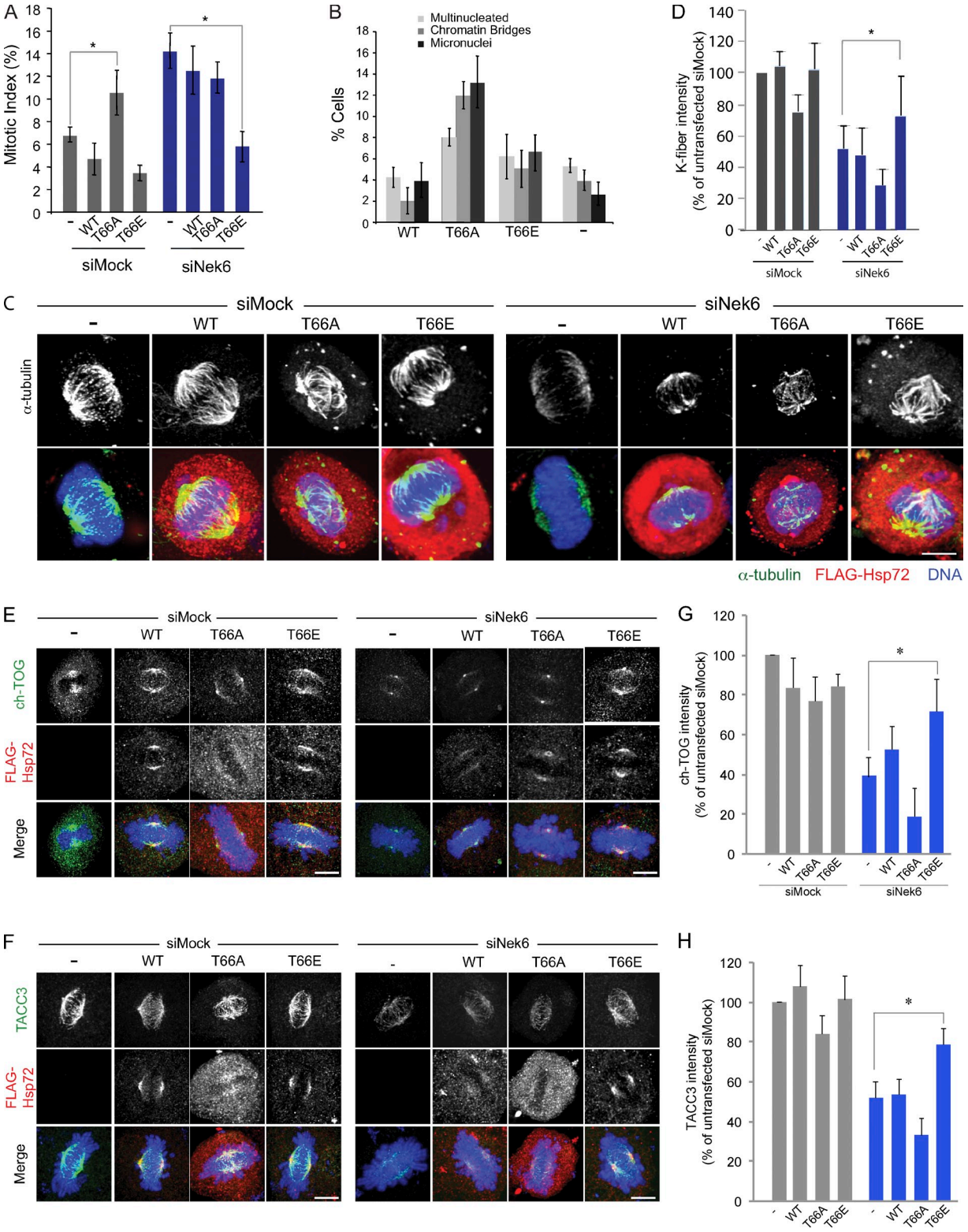

Figure 5. **Hsp72-T66E rescues mitotic defects that arise upon Nek6 depletion.** (A) HeLa cells were mock or Nek6 depleted for 48 h before transfection with Flag-Hsp72 constructs as indicated for 24 h and IF with Flag and phospho-H3 antibodies. The mitotic index of transfected cells was counted by microscopic analysis of chromatin. (B) HeLa cells transfected with Flag-Hsp72 constructs indicated for 24 h were stained with Flag and α-tubulin antibodies and scored by IF for the occurrence of nuclear defects. Data in A and B are means (±SD) of 100–300 cells. (C) HeLa cells were treated as in A, placed on ice for 10 min, and analyzed by IF with antibodies against α-tubulin to reveal K-fibers (green) and Flag to detect transfected cells. (D) Total K-fiber intensity from C is plotted relative to that in mock-treated samples. (E and F) HeLa cells were treated and processed as in C but with ch-TOG (E) and TACC3 (F) antibodies. (G and H) Total ch-TOG and TACC3 intensity from E and F is plotted relative to that in mock-treated samples. Error bars show means ± SD. In C, E, and F, DNA was stained with Hoechst 33258 (blue). siMock, mock siRNA; WT, wild type. *, $P < 0.05$. Bars, 10 µm.

(Neckers and Workman, 2012). Hsp90 works in concert with Hsp70, and dual depletion of Hsc70 and Hsp72 blocks not only Hsp90 function but also the Hsp70-mediated inhibition of apoptosis that can otherwise confer resistance to Hsp90 inhibitors (Powers et al., 2008). Hence, considerable effort is now being put into development of Hsp70 inhibitors (Leu et al., 2009; Patury et al., 2009; Massey et al., 2010; Powers et al., 2010; Balaburski et al., 2013; Budina-Kolomets et al., 2014). Non–cancer-derived cells tend to have reduced transcription of Hsp72 in mitosis (Martínez-Balbás et al., 1995). This results from HSF2 (heat shock factor 2) acting as a transcriptional repressor in mitosis, blocking expression of Hsp72 by HSF1. However, in some cancer cells, HSF2 is repressed in mitosis, allowing HSF1 to maintain elevated Hsp72 (Elsing et al., 2014). The dependence on Hsp72 that this implies may provide a therapeutic window for targeted inhibitors in these cancer types. Hsp72 is a novel mitotic substrate of Nek6, and there is growing support for Nek6 as an anticancer target (Capra et al., 2006; Chen et al., 2006; Takeno et al., 2008; Nassirpour et al., 2010). The efficacy of Hsp70 inhibitors, both as single agents and in combination with Hsp90 or Nek6 inhibitors, will be exciting to test in different cancer settings.

Materials and methods

KESTREL analysis

600 confluent 15-cm dishes of HEK 293 cells were collected, washed in PBS, and lysed in 50 mM Tris.HCl, pH 7.5, 5% glycerol, 14 mM 2-mercaptoethanol, 2 mM EDTA, 2 mM EGTA, 10 µg/ml aprotinin, 10 µg/ml leupeptin, and 1 mM Pefabloc. Insoluble material was sedimented by centrifugation at 15,000 *g* for 25 min at 4°C. The supernatant was filtered and degassed through a Stericup vacuum filter and then desalted, and buffer was exchanged into MOPS–low salt buffer (LSB; 30 mM MOPS, pH 7.0, 5% glycerol, 7 mM 2-mercaptoethanol, and 0.03% Brij) by chromatography over a 480-ml Sephadex G-25 fine column. The desalted extract was applied to a 25-ml Heparin Sepharose High Performance column. The column was washed in 125 ml MOPS-LSB and then eluted over a 400-ml gradient to 1.2 M NaCl in MOPS-LSB while 40 10-ml fractions were collected. 20 µl of each fraction were diluted 1:10 in KESTREL test buffer (50 mM Tris.HCl, pH 7.5, 7 mM 2-mercaptoethanol, 1 mM EGTA, 10 µg/ml leupeptin, and 1 mM Pefabloc) and incubated for 5 min with 3 mM $MnCl_2$ and 1 kBq/ml γ-[^{32}P]ATP in the absence or presence of 1 µg/ml active recombinant Nek6 (Invitrogen). Reaction products were analyzed by SDS-PAGE, transfer to Immobilon P (EMD Millipore), and subsequent autoradiography. Heparin Sepharose fractions 16–18 contained potential Nek6 substrates and so were pooled, desalted, separated along a 10-ml gradient to 1 M NaCl on a 1-ml Source 15Q column, and analyzed for potential Nek6 substrates as described in the previous paragraph. Substrate containing Source 15Q fractions 16–18 were pooled, separated by size using a 120 ml Superdex 200 column, and analyzed as in this paragraph. Superdex 200 fractions 3–7 were pooled, concentrated by filtration, and incubated with either 3 mM $MnCl_2$ or 10 mM Mg-acetate in the presence of γ-[^{32}P]ATP, with or without 1 µg/ml Nek6. The reactions were denatured, alkylated with 50 mM iodoacetamide, and separated by SDS-PAGE, and the gels were stained with colloidal Coomassie (Invitrogen) and subsequently analyzed by autoradiography. Protein bands that were visible with Coomassie staining and had been radiolabeled in the presence of Nek6 were excised from the gels, destained, digested with trypsin, and subjected to mass spectrometry fingerprinting (matrix-assisted laser desorption/ionization–tandem time of flight) using a proteomics analyzer (4700; Applied Biosystems) for data acquisition and the Mascot search engine (Matrix Science) to search for matches in the NCBInr database.

Plasmid construction, mutagenesis, and recombinant protein expression

Full-length cDNAs expressing human Hsp72 and Hsc70, provided by R. van Monfort (Institute of Cancer Research, Sutton, England, UK), were amplified by PCR and inserted into pLEICS-12 for expression with an N-terminal Flag tag from a constitutive cytomegalovirus promoter in mammalian cells. They were also subcloned into the pTWO-E plasmid, expressed as His fusions from a T7 promoter, and purified on 5-ml HisTrap columns (GE Healthcare); columns were washed with 50 mM imidazole, and protein was eluted on a gradient of 50–500 mM imidazole. The eluted protein was dialyzed against 20 mM Tris, pH 8.0, 100 mM NaCl, and 5 mM β-mercaptoethanol and passed over a 5-ml Q Sepharose column to remove contamination by the *Escherichia coli* Hsp70 homologue DnaK. The Q column flow-through was dialyzed into 100 mM Tris, pH 7.5, 150 mM NaCl, 6 mM $MgCl_2$, and 10% glycerol and concentrated to 5 mg/ml. The absence of DnaK from Hsp70 samples was confirmed by Western blotting with SPA-880 mouse antibody (Enzo Life Sciences). Flag-Nek6 and Flag-Nek7 plasmids are as previously described (O'Regan and Fry, 2009). In brief, full-length cDNAs of Nek6 and Nek7 were subcloned into the pFLAG-CMV2 vector as PCR fragments using NotI and XbaI sites. Flag-TACC3 was inserted into pTre2Hyg by subcloning a Flag-TACC3 PCR fragment with NheI and NotI sites. Mutations were introduced using the GeneTailor Site-Directed Mutagenesis System (Invitrogen), and all constructs were confirmed by Sanger sequencing.

Cell culture, synchronization, and transfection

HeLa and HEK 293 cells were grown in DMEM (Invitrogen) supplemented with 10% heat-inactivated FBS, 100 IU/ml penicillin, and 100 µg/ml streptomycin at 37°C in a 5% CO_2 atmosphere. For inducible expression of Flag-TACC3, TetOn HeLa cells (Takara Bio Inc.) were used. TetOn HeLa cells with stably integrated pTRE2hyg-Flag-TACC3 plasmid were maintained with 300 µg/ml G418 and 200 µg/ml Hygromycin B. Expression of Flag-TACC3 was induced with 0.5 µg/ml doxycycline, 24 h before analysis. Cells were synchronized in S phase by incubation for 16 h with either 1 mM hydroxyurea or 2 mM thymidine. M-phase arrested cells were prepared by shake-off after 16 h treatment with either 50 ng/ml nocodazole or 100 µM monastrol. For G1 cells, a mitotic population was collected as described for M phase–arrested cells and replaced into fresh medium for 6 h. G2 cells were obtained by placing thymidine-treated cells into fresh medium for 8 h. Synchronization was confirmed by flow cytometry. To reveal K-fibers, synchronized cells were replaced into chilled media and incubated on ice for 10 min before methanol fixation. For IPs from mitotic cells, nocodazole was washed out, and cells were replaced into fresh media for 45 min to allow spindle MTs to form before cell lysis. Transient transfections were performed with FuGENE HD reagent (Promega) according to manufacturer's instructions, and cells were transfected for 24 h, unless stated otherwise. To inhibit Hsp70, cells were treated with 5 µM VER-155008 (Tocris Bioscience) for 4 h; control cells were treated with the same volume of DMSO. To depolymerase MTs, cells were incubated with 3 µM nocodazole for 4 h. HeLa-EGFP-LaminA/mCherry-H2B cells were provided by J. Ellenberg (European Molecular Biology Laboratory, Heidelberg, Germany) and grown in DMEM supplemented with 10% FBS, 500 µg/ml G418, and 0.5 µg/ml puromycin.

Fixed and live-cell microscopy

Cells grown on acid-etched glass coverslips were fixed with ice-cold methanol and processed as previously described (O'Regan and Fry, 2009). In brief, media were aspirated, and cells were fixed by incubation in ice-cold methanol at −20°C for a minimum of 10 min. Cells were then blocked in PBS supplemented with 3% BSA before incubation with the appropriate antibody diluted as required in PBS supplemented with 3% BSA. For Hsp72 staining, cells were preextracted for 30 s (60 mM Pipes, 25 mM Hepes, pH 7.4, 10 mM EGTA, 2 mM $MgCl_2$, and 1% Triton X-100) before methanol fixation, whereas for ch-TOG and TACC3 staining, cells were fixed in 3.7% formaldehyde and permeabilized with 0.5% Triton X-100. Primary antibodies were 1 µg/ml mouse Hsp72 (Enzo Life Sciences), 0.3 µg/ml mouse α-tubulin (Sigma-Aldrich), 2 µg/ml rabbit α-tubulin (Abcam), 0.5 µg/ml mouse Flag (Sigma-Aldrich), 2 µg/ml mouse phospho–histone H3 (EMD Millipore), 2 µg/ml mouse CenpA (Abcam), 1 µg/ml rabbit ch-TOG (Bethyl Laboratories, Inc.), 2 µg/ml mouse TACC3 (Abcam), 1 µg/ml mouse BubR1 (EMD Millipore), 0.5 µg/ml rabbit GFP (Abcam), 1 µg/ml mouse CenpE (Santa Cruz Biotechnology, Inc.), 2 µg/ml rabbit Nek6 (O'Regan and Fry, 2009), and 1 µg/ml rabbit pHsp70 (this study). Nek6 antibodies were raised against a peptide corresponding to amino acids 1–15 conjugated to keyhole limpet hemocyanin via an N-terminal cysteine (C-MAQPGHMPHGGSSN), whereas Hsp70 antibodies were raised against a phosphopeptide corresponding to amino acid residues 60–72 conjugated to ovalbumin via a C-terminal cysteine (ALNPQNT(p)VFDAKR-C). Secondary antibodies used were Alexa Fluor 488 and 594 goat anti–rabbit and goat anti–mouse IgGs (1 µg/ml; Invitrogen).

Imaging was performed on a confocal microscope (TCS SP5; Leica) equipped with an inverted microscope (DMI6000 B; Leica) using a 63× oil objective (numerical aperture, 1.4). Z stacks comprising 30–50 0.3-µm sections were acquired using LAS-AF software (Leica), and deconvolution of 3D image stacks were performed using Huygens software (Scientific Volume Imaging). To quantify spindle and K-fiber MTs, the mean pixel intensity of the α-tubulin antibody signal over a half-spindle was measured, and cytoplasmic background was subtracted. Intensities were scaled so that the control intensity was 100%. To quantify recruitment of TACC3 and ch-TOG, the mean pixel intensity over a half-spindle was measured in both the spindle and TACC3 or ch-TOG channels, and cytoplasmic background was subtracted. The intensity of TACC3 or ch-TOG was then normalized to the spindle intensity.

Time-lapse imaging was performed on a confocal microscope (TCS SP5) equipped with an inverted microscope (DMI6000 B) using a 63× oil objective (numerical aperture, 1.4). Cells were cultured in glass-bottomed dishes (MatTek Corporation) and maintained on the stage at 37°C in an atmosphere supplemented with 5% CO_2 using a microscope temperature control system (Life Imaging Services). Z stacks comprising 20 0.5-µm sections were acquired every 10 min for ≥18 h using LAS-AF software. Stacks were converted into maximum intensity projections using LAS-AF software, and videos were prepared using ImageJ (National Institutes of Health).

IP and kinase assays

Cells were harvested by incubation with PBS + 0.5 mM EDTA and pelleted by centrifugation before being lysed in Nek extraction buffer (Fry and Nigg, 1997). Antibodies used to perform IPs were 2 µg/ml rabbit Nek6 (O'Regan and Fry, 2009), 0.5 µg/ml mouse FLAG (Sigma-Aldrich), or 2 µg/ml mouse Hsp72 (Enzo Life Sciences). Control IPs were performed with rabbit or mouse IgGs (Sigma-Aldrich), as appropriate, at the same concentration. Kinase assays were performed using either 5–10 µl of washed immune complex beads or 0.1 µg of purified kinase. Proteins were incubated with 5 µg of substrate and 1 µCi γ-[^{32}P]ATP in 40 µl kinase buffer (50 mM Hepes.KOH, pH 7.4, 5 mM $MnCl_2$, 5 mM β-glycerophosphate, 5 mM NaF, 4 µM ATP, and 1 mM DTT) at 30°C for 30 min. Reactions were stopped with 50 µl of protein sample buffer and analyzed by SDS-PAGE and autoradiography. Substrate phosphorylation was quantified by scintillation counting of proteins excised from dried gels. Proteins that coprecipitated with and were phosphorylated by Nek6 were excised from gels and subjected to mass spectrometry fingerprinting (University of Leicester, Leicester, England, UK).

RNAi

Cells at 30–40% confluency were cultured in Opti-MEM Reduced Serum Medium and transfected with 50 nM ON-TARGETplus siRNA duplexes using Oligofectamine (Invitrogen) according to the manufacturer's instructions. siRNA duplexes were as follows: Hsp72, J-005168-06, -07, and -08; Nek6, J-004166-06 and J-004166-09; Nek7, J-003795-12 (all obtained from Thermo Fisher Scientific); and GAPDH (4390850; Life Technologies). 72 h after transfection, cells were either fixed for immunocytochemistry or prepared for IP, Western blot, or flow cytometry analysis.

Phosphomapping and phosphoantibody generation

For phosphosite mapping, Hsp72 purified from HEK293 cells or bacterially expressed recombinant Hsp72 was incubated with Nek6 as described under IP and kinase assays. Proteins were then separated by SDS-PAGE, excised, reduced with 1 mM Tris (2-carboxyethyl) phosphine, alkylated with 50 mM iodoacetamide, digested with trypsin, extracted, and subjected to analysis by nano–liquid chromatography–tandem mass spectrometry precursor ion scanning (searching for peptides that have lost 79 D, equivalent to PO_3^-) on a quadrupole-linear ion trap mass spectrometer (4000 Q-Trap; Applied Biosystems; McCoy et al., 2007). For production of Hsp70-pT66 antibodies, rabbits were immunized with peptides representing residues 60–72 with a modified T66 coupled to ovalbumin via a C-terminal cysteine (made by Peptide Specialty Laboratories, GmbH). Antibodies were purified by sequential passage over columns containing, first, the nonphosphorylated peptide collecting the flow-through and, second, the phosphorylated peptide. Columns were washed extensively with 10 mM sodium phosphate, pH 6.8, and specific antibodies were eluted with 0.1 M glycine, pH 2.4, containing neutralizing quantities of 2 M K_2HPO_4.

Cell lysis and Western blotting

Cell lysis, SDS-PAGE, and Western blotting were as previously described (Hames et al., 2005). For Western blotting, primary antibodies used were 1 µg/ml rabbit Nek6 (O'Regan and Fry, 2009), 1 µg/ml rabbit Nek7 (O'Regan and Fry, 2009), 0.3 µg/ml mouse α-tubulin (Sigma-Aldrich), 0.5 µg/ml mouse Flag (Sigma-Aldrich), 0.5 µg/ml mouse Hsp70 (Santa Cruz Biotechnology, Inc.), 0.5 µg/ml mouse Hsp72 (Enzo Life Sciences), 0.5 µg/ml mouse Hsc70 (Santa Cruz Biotechnology, Inc.), 1 µg/ml rabbit pHsp70 (this study), 0.8 µg/ml goat Nek9 (Santa Cruz Biotechnology, Inc.), 1 µg/ml rabbit GAPDH (Cell Signaling Technology), 1 µg/ml mouse phospho–histone H3 (EMD Millipore), 0.2 µg/ml rabbit γ-tubulin (Sigma-Aldrich), 0.4 µg/ml mouse TACC3 (Abcam), 0.5 µg/ml rabbit ch-TOG (Bethyl Laboratories, Inc.), and 1 µg/ml mouse Cep55 (Santa Cruz Biotechnology, Inc.). Nek7 antibodies were raised against a peptide corresponding to amino acid residues 12–28 conjugated to keyhole limpet hemocyanin via an N-terminal cysteine (C-OVPQFQPQKALRPDM). Secondary antibodies were HRP-labeled anti–mouse, anti–rabbit, or anti–goat IgGs (1:1,000; Sigma-Aldrich) or alkaline phosphatase–conjugated IgGs (1:7,500; Promega). HRP-labeled blots were detected by enhanced chemiluminescence (Thermo Fisher Scientific).

Statistical analysis

All quantitative data represent means and SD of at least three independent experiments. Statistical analyses were performed using a one-tailed unpaired Student's *t* test assuming unequal variance, a one-way analysis of variance followed by post hoc testing or an χ^2 test, as appropriate. P-values represent *, $P < 0.05$; **, $P < 0.01$; ***, $P < 0.001$. For box and whisker plots, boxes represent the 25th and 75th percentile, the green and white lines represent the medians and means, respectively, and whiskers show the 10th and 90th percentile.

Online supplemental material

Fig. S1 shows purification of Nek6 substrates from HEK293 extracts using the KESTREL strategy. Fig. S2 shows additional data relating to mitotic phenotypes associated with loss of Hsp72 activity. Fig. S3 shows mapping of the Nek6 phosphorylation site on Hsp72 and the validation of Hsp72pT66 antibody specificity when used for immunofluorescence (IF). Videos 1–3 show time-lapse imaging of chromosome congression in control, Hsp72-depleted, and Hsp70i-treated cells, respectively. Videos 4 and 5 show time-lapse imaging of metaphase chromosome alignment in DMSO- or Hsp70i-treated cells, respectively. Online supplemental material is available at http://www.jcb.org/cgi/content/full/jcb.201409151/DC1.

We thank J. Ellenberg (University of Heidelberg) and R. van Montfort (University of Sutton) for reagents and D. Lamont and K. Beattie (University of Dundee), as well as the University of Leicester Core Biotechnology Services, for technical support and access to core facilities.

This work was funded by grants from Worldwide Cancer Research (13-0042), Cancer Research UK (C1362/A18081; C24461/A12772; C25425/A15182), The Wellcome Trust (082828; 097828), the Lister Institute of Preventive Medicine, and a joint PhD studentship from the Medical Research Council and Hope Against Cancer.

The authors declare no competing financial interests.

Submitted: 30 September 2014
Accepted: 31 March 2015

References

Balaburski, G.M., J.I. Leu, N. Beeharry, S. Hayik, M.D. Andrake, G. Zhang, M. Herlyn, J. Villanueva, R.L. Dunbrack Jr., T. Yen, et al. 2013. A modified HSP70 inhibitor shows broad activity as an anticancer agent. *Mol. Cancer Res.* 11:219–229. http://dx.doi.org/10.1158/1541-7786.MCR-12-0547-T

Booth, D.G., F.E. Hood, I.A. Prior, and S.J. Royle. 2011. A TACC3/ch-TOG/clathrin complex stabilises kinetochore fibres by inter-microtubule bridging. *EMBO J.* 30:906–919. http://dx.doi.org/10.1038/emboj.2011.15

Budina-Kolomets, A., G.M. Balaburski, A. Bondar, N. Beeharry, T. Yen, and M.E. Murphy. 2014. Comparison of the activity of three different HSP70 inhibitors on apoptosis, cell cycle arrest, autophagy inhibition, and HSP90 inhibition. *Cancer Biol. Ther.* 15:194–199. http://dx.doi.org/10.4161/cbt.26720

Bukau, B., J. Weissman, and A. Horwich. 2006. Molecular chaperones and protein quality control. *Cell.* 125:443–451. http://dx.doi.org/10.1016/j.cell.2006.04.014

Capra, M., P.G. Nuciforo, S. Confalonieri, M. Quarto, M. Bianchi, M. Nebuloni, R. Boldorini, F. Pallotti, G. Viale, M.L. Gishizky, et al. 2006. Frequent alterations in the expression of serine/threonine kinases in human cancers. *Cancer Res.* 66:8147–8154. http://dx.doi.org/10.1158/0008-5472.CAN-05-3489

Chen, J., L. Li, Y. Zhang, H. Yang, Y. Wei, L. Zhang, X. Liu, and L. Yu. 2006. Interaction of Pin1 with Nek6 and characterization of their expression correlation in Chinese hepatocellular carcinoma patients. *Biochem. Biophys. Res. Commun.* 341:1059–1065. http://dx.doi.org/10.1016/j.bbrc.2005.12.228

Cohen, P., and A. Knebel. 2006. KESTREL: a powerful method for identifying the physiological substrates of protein kinases. *Biochem. J.* 393:1–6. http://dx.doi.org/10.1042/BJ20051545

Daugaard, M., M. Rohde, and M. Jäättelä. 2007. The heat shock protein 70 family: Highly homologous proteins with overlapping and distinct functions. *FEBS Lett.* 581:3702–3710. http://dx.doi.org/10.1016/j.febslet.2007.05.039

Elsing, A.N., C. Aspelin, J.K. Björk, H.A. Bergman, S.V. Himanen, M.J. Kallio, P. Roos-Mattjus, and L. Sistonen. 2014. Expression of HSF2 decreases in mitosis to enable stress-inducible transcription and cell survival. *J. Cell Biol.* 206:735–749. http://dx.doi.org/10.1083/jcb.201402002

Fry, A.M., and E.A. Nigg. 1997. Characterization of mammalian NIMA-related kinases. *Methods Enzymol.* 283:270–282. http://dx.doi.org/10.1016/S0076-6879(97)83022-4

Fry, A.M., L. O'Regan, S.R. Sabir, and R. Bayliss. 2012. Cell cycle regulation by the NEK family of protein kinases. *J. Cell Sci.* 125:4423–4433. http://dx.doi.org/10.1242/jcs.111195

Hames, R.S., R.E. Crookes, K.R. Straatman, A. Merdes, M.J. Hayes, A.J. Faragher, and A.M. Fry. 2005. Dynamic recruitment of Nek2 kinase to the centrosome involves microtubules, PCM-1, and localized proteasomal degradation. *Mol. Biol. Cell.* 16:1711–1724. http://dx.doi.org/10.1091/mbc.E04-08-0688

Hood, F.E., S.J. Williams, S.G. Burgess, M.W. Richards, D. Roth, A. Straube, M. Pfuhl, R. Bayliss, and S.J. Royle. 2013. Coordination of adjacent domains mediates TACC3–ch-TOG–clathrin assembly and mitotic spindle binding. *J. Cell Biol.* 202:463–478. http://dx.doi.org/10.1083/jcb.201211127

Hut, H.M., H.H. Kampinga, and O.C. Sibon. 2005. Hsp70 protects mitotic cells against heat-induced centrosome damage and division abnormalities. *Mol. Biol. Cell.* 16:3776–3785. http://dx.doi.org/10.1091/mbc.E05-01-0038

Jego, G., A. Hazoumé, R. Seigneuric, and C. Garrido. 2013. Targeting heat shock proteins in cancer. *Cancer Lett.* 332:275–285. http://dx.doi.org/10.1016/j.canlet.2010.10.014

Kampinga, H.H., and E.A. Craig. 2010. The HSP70 chaperone machinery: J proteins as drivers of functional specificity. *Nat. Rev. Mol. Cell Biol.* 11:579–592. http://dx.doi.org/10.1038/nrm2941

Leu, J.I., J. Pimkina, A. Frank, M.E. Murphy, and D.L. George. 2009. A small molecule inhibitor of inducible heat shock protein 70. *Mol. Cell.* 36:15–27. http://dx.doi.org/10.1016/j.molcel.2009.09.023

Liang, P., and T.H. MacRae. 1997. Molecular chaperones and the cytoskeleton. *J. Cell Sci.* 110:1431–1440.

Mack, G.J., and D.A. Compton. 2001. Analysis of mitotic microtubule-associated proteins using mass spectrometry identifies astrin, a spindle-associated protein. *Proc. Natl. Acad. Sci. USA.* 98:14434–14439. http://dx.doi.org/10.1073/pnas.261371298

Martínez-Balbás, M.A., A. Dey, S.K. Rabindran, K. Ozato, and C. Wu. 1995. Displacement of sequence-specific transcription factors from mitotic chromatin. *Cell.* 83:29–38. http://dx.doi.org/10.1016/0092-8674(95)90231-7

Massey, A.J., D.S. Williamson, H. Browne, J.B. Murray, P. Dokurno, T. Shaw, A.T. Macias, Z. Daniels, S. Geoffroy, M. Dopson, et al. 2010. A novel, small molecule inhibitor of Hsc70/Hsp70 potentiates Hsp90 inhibitor induced apoptosis in HCT116 colon carcinoma cells. *Cancer Chemother. Pharmacol.* 66:535–545. http://dx.doi.org/10.1007/s00280-009-1194-3

McCoy, C.E., A. macdonald, N.A. Morrice, D.G. Campbell, M. Deak, R. Toth, J. McIlrath, and J.S. Arthur. 2007. Identification of novel phosphorylation sites in MSK1 by precursor ion scanning MS. *Biochem. J.* 402:491–501. http://dx.doi.org/10.1042/BJ20061183

Moniz, L., P. Dutt, N. Haider, and V. Stambolic. 2011. Nek family of kinases in cell cycle, checkpoint control and cancer. *Cell Div.* 6:18. http://dx.doi.org/10.1186/1747-1028-6-18

Murphy, M.E. 2013. The HSP70 family and cancer. *Carcinogenesis.* 34:1181–1188. http://dx.doi.org/10.1093/carcin/bgt111

Nassirpour, R., L. Shao, P. Flanagan, T. Abrams, B. Jallal, T. Smeal, and M.J. Yin. 2010. Nek6 mediates human cancer cell transformation and is a potential cancer therapeutic target. *Mol. Cancer Res.* 8:717–728. http://dx.doi.org/10.1158/1541-7786.MCR-09-0291

Neckers, L., and P. Workman. 2012. Hsp90 molecular chaperone inhibitors: are we there yet? *Clin. Cancer Res.* 18:64–76. http://dx.doi.org/10.1158/1078-0432.CCR-11-1000

Nylandsted, J., M. Rohde, K. Brand, L. Bastholm, F. Elling, and M. Jäättelä. 2000. Selective depletion of heat shock protein 70 (Hsp70) activates a tumor-specific death program that is independent of caspases and bypasses Bcl-2. *Proc. Natl. Acad. Sci. USA.* 97:7871–7876. http://dx.doi.org/10.1073/pnas.97.14.7871

O'Connell, M.J., M.J. Krien, and T. Hunter. 2003. Never say never. The NIMA-related protein kinases in mitotic control. *Trends Cell Biol.* 13:221–228. http://dx.doi.org/10.1016/S0962-8924(03)00056-4

O'Regan, L., and A.M. Fry. 2009. The Nek6 and Nek7 protein kinases are required for robust mitotic spindle formation and cytokinesis. *Mol. Cell. Biol.* 29:3975–3990. http://dx.doi.org/10.1128/MCB.01867-08

Patury, S., Y. Miyata, and J.E. Gestwicki. 2009. Pharmacological targeting of the Hsp70 chaperone. *Curr. Top. Med. Chem.* 9:1337–1351. http://dx.doi.org/10.2174/156802609789895674

Powers, M.V., and P. Workman. 2007. Inhibitors of the heat shock response: biology and pharmacology. *FEBS Lett.* 581:3758–3769. http://dx.doi.org/10.1016/j.febslet.2007.05.040

Powers, M.V., P.A. Clarke, and P. Workman. 2008. Dual targeting of HSC70 and HSP72 inhibits HSP90 function and induces tumor-specific apoptosis. *Cancer Cell.* 14:250–262. http://dx.doi.org/10.1016/j.ccr.2008.08.002

Powers, M.V., K. Jones, C. Barillari, I. Westwood, R.L. van Montfort, and P. Workman. 2010. Targeting HSP70: the second potentially druggable heat shock protein and molecular chaperone? *Cell Cycle.* 9:1542–1550. http://dx.doi.org/10.4161/cc.9.8.11204

Quarmby, L.M., and M.R. Mahjoub. 2005. Caught Nek-ing: cilia and centrioles. *J. Cell Sci.* 118:5161–5169. http://dx.doi.org/10.1242/jcs.02681

Rapley, J., M. Nicolàs, A. Groen, L. Regué, M.T. Bertran, C. Caelles, J. Avruch, and J. Roig. 2008. The NIMA-family kinase Nek6 phosphorylates the kinesin Eg5 at a novel site necessary for mitotic spindle formation. *J. Cell Sci.* 121:3912–3921. http://dx.doi.org/10.1242/jcs.035360

Rérole, A.L., J. Gobbo, A. De Thonel, E. Schmitt, J.P. Pais de Barros, A. Hammann, D. Lanneau, E. Fourmaux, O. Deminov, O. Micheau, et al. 2011. Peptides and aptamers targeting HSP70: a novel approach for anticancer chemotherapy. *Cancer Res.* 71:484–495. http://dx.doi.org/10.1158/0008-5472.CAN-10-1443

Richards, M.W., L. O'Regan, C. Mas-Droux, J.M. Blot, J. Cheung, S. Hoelder, A.M. Fry, and R. Bayliss. 2009. An autoinhibitory tyrosine motif in the cell-cycle-regulated Nek7 kinase is released through binding of Nek9. *Mol. Cell.* 36:560–570. http://dx.doi.org/10.1016/j.molcel.2009.09.038

Rohde, M., M. Daugaard, M.H. Jensen, K. Helin, J. Nylandsted, and M. Jäättelä. 2005. Members of the heat-shock protein 70 family promote cancer cell growth by distinct mechanisms. *Genes Dev.* 19:570–582. http://dx.doi.org/10.1101/gad.305405

Roig, J., A. Mikhailov, C. Belham, and J. Avruch. 2002. Nercc1, a mammalian NIMA-family kinase, binds the Ran GTPase and regulates mitotic progression. *Genes Dev.* 16:1640–1658. http://dx.doi.org/10.1101/gad.972202

Sauer, G., R. Körner, A. Hanisch, A. Ries, E.A. Nigg, and H.H. Silljé. 2005. Proteome analysis of the human mitotic spindle. *Mol. Cell. Proteomics.* 4:35–43. http://dx.doi.org/10.1074/mcp.M400158-MCP200

Schmitt, E., L. Maingret, P.E. Puig, A.L. Rerole, F. Ghiringhelli, A. Hammann, E. Solary, G. Kroemer, and C. Garrido. 2006. Heat shock protein 70 neutralization exerts potent antitumor effects in animal models of colon cancer and melanoma. *Cancer Res.* 66:4191–4197. http://dx.doi.org/10.1158/0008-5472.CAN-05-3778

Takeno, A., I. Takemasa, Y. Doki, M. Yamasaki, H. Miyata, S. Takiguchi, Y. Fujiwara, K. Matsubara, and M. Monden. 2008. Integrative approach for differentially overexpressed genes in gastric cancer by combining large-scale gene expression profiling and network analysis. *Br. J. Cancer.* 99:1307–1315. http://dx.doi.org/10.1038/sj.bjc.6604682

Vaz Meirelles, G., D.C. Ferreira Lanza, J.C. da Silva, J. Santana Bernachi, A.F. Paes Leme, and J. Kobarg. 2010. Characterization of hNek6 interactome reveals an important role for its short N-terminal domain and colocalization with proteins at the centrosome. *J. Proteome Res.* 9:6298–6316. http://dx.doi.org/10.1021/pr100562w

Yin, M.-J., L. Shao, D. Voehringer, T. Smeal, and B. Jallal. 2003. The serine/threonine kinase Nek6 is required for cell cycle progression through mitosis. *J. Biol. Chem.* 278:52454–52460. http://dx.doi.org/10.1074/jbc.M308080200